

Nanoscale x-ray absorption spectroscopy using XEOL-SNOM detection mode

**D Pailharey¹, Y Mathey¹, F Jandard¹, S Larcheri², F Rocca², A Kuzmin³,
R Kalendarev³, J Purans³, G Dalba⁴, R Graziola⁴ and O Dhez⁵**

¹ CRMCN-CNRS, UPR 7251 - Université de la Méditerranée, Marseille, France

² IFN-CNR Section "CeFSA" of Trento, Povo (Trento), Italy

³ Institute of Solid State Physics, University of Latvia, Riga, Latvia

⁴ Department of Physics, Povo (Trento), Italy

⁵ INFN-CNR, c/o ESRF, Grenoble, France

E-mail: pailharey@crmcn.univ-mrs.fr, rocca@science.unitn.it, a.kuzmin@cfi.lu.lv

Abstract. The first results obtained with the prototype system at the synchrotron beamline ID03 at ESRF are presented and illustrate the possibility to detect an element-specific contrast and to perform nanoscale x-ray absorption spectroscopy experiments at the Zn K and W L₃ absorption edges in mixed zinc oxide-zinc tungstate thin films.

1. Introduction

Investigations of complex nanostructured materials used in modern technologies require special experimental techniques able to provide an information on the structure and electronic properties of the materials with spatial resolution down to the nanometre range. X-ray absorption spectroscopy (XAS) using synchrotron radiation is one of the powerful structural methods probing local environment around a particular element [1]. On macroscopic scale, several detection methods have been developed in the past to register the x-ray absorption signal across the element absorption edge [2,3] using conventional transmission technique, fluorescence, total electron yield (TEY) or x-ray excited optical luminescence (XEOL), etc. Further improvements have been done by combining XAS with x-ray optics able to reduce the beam size to the sub-microscale. The microfocusing optics in hard x-ray region, largely used for XAS, are represented by Kirkpatrick-Baez systems [4,5], capillaries [6,7], waveguides [8], Fresnel zone plates [9] and refractive lenses [10]. Today such optical devices are used in two types of spectromicroscopy techniques [3] - scanning transmission x-ray microscopy (STXRM), based on photon detection, and scanning photoemission electron microscopy (SPEEM), utilizing electron detection.

In this work, we present a new experimental set-up based on a combination of XAS using synchrotron radiation microbeam with scanning near-field optical microscopy (SNOM) [11] detection of XEOL signal. The new instrumentation, developed within the EC FP6 "X-TIP" project, merges the ability of XAS in providing structural information, elemental composition and chemical status of specific element with the lateral resolution and surface morphology sensitivity of SNOM. Further, we will present and discuss the first results, obtained with the prototype system at the ESRF synchrotron beamline ID03, which illustrate the possibility to obtain an element-specific contrast and to perform

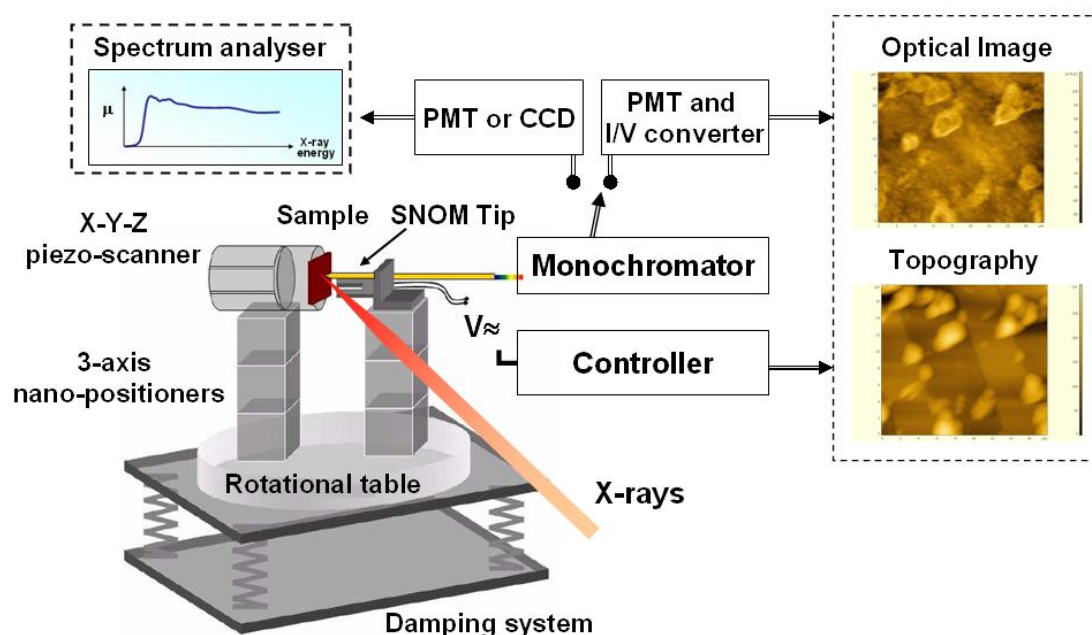


Figure 1 (Colour online) Schematic view of the XAS-SNOM experimental setup.

nanoscale-XAS experiments by detecting the Zn K and W L₃ absorption edges in ZnO-ZnWO₄ thin films.

2. Experimental

Mixed thin film samples of ZnO-ZnWO₄ were prepared by dc magnetron co-sputtering technique from metallic zinc (99.9%) and tungsten (99.95%) targets in mixed argon(80%)-oxygen(20%) atmosphere. The films with the thickness about 300 nm were deposited on silicon substrates and annealed in air at 900°C for 8 h. The presence of two (ZnO and ZnWO₄) phases in the films was evidenced by x-ray diffraction and micro-Raman spectroscopy. Green photoluminescence, peaked at about 500 nm, was observed in all samples under x-ray excitation: this broadband emission originates from a superposition of two bands due to ZnO (~530 nm) and ZnWO₄(~500 nm) phases.

Synchrotron radiation measurements were performed at the ESRF (Grenoble, France) storage ring, operated at 6 GeV and 200 mA, using our XAS-SNOM prototype system (figure 1). The ID03 beamline, equipped with the channel-cut Si(111) monochromator and Kirkpatrick-Baez (KB) focusing optics, was used as a microfocusing x-ray source. The monochromatic x-ray beam, scanning in the energy range from 9600 eV to 10400 eV, was used to excite the XEOL signal across the Zn K-edge (at 9659 eV) and W L₃-edge (at 10207 eV). The size of the micro-beam at the sample was 18×24 μm². The estimated x-ray flux value at 9700 eV was 3.4·10¹² photons/s, and the x-ray density was 5.6·10⁹ photons/s/μm².

Our XAS-SNOM prototype system (figure 1) consists of an autoexcited quartz-tuning fork head, mounted on nanopositioning system; a sharpened and coated optical fibre, operating as a probe in shear-force near-field mode; a detection system (a spectrometer with CCD detector for fast spectral analysis of XEOL signals or an analogue PMT detector for imaging), coupled with the head control system; software/hardware for synchronization of SNOM signal detection with synchrotron beamline acquisition system. The lateral resolution of the prototype was tip dependent but commonly details down to 100 nm are visible.

Two types of experiments were performed at room temperature. In the first one, the SNOM probe was used to image the sample surface topography; after that, the probe was placed in a point of interest and kept at the same position in near-field condition while the x-ray energy was tuned across the Zn

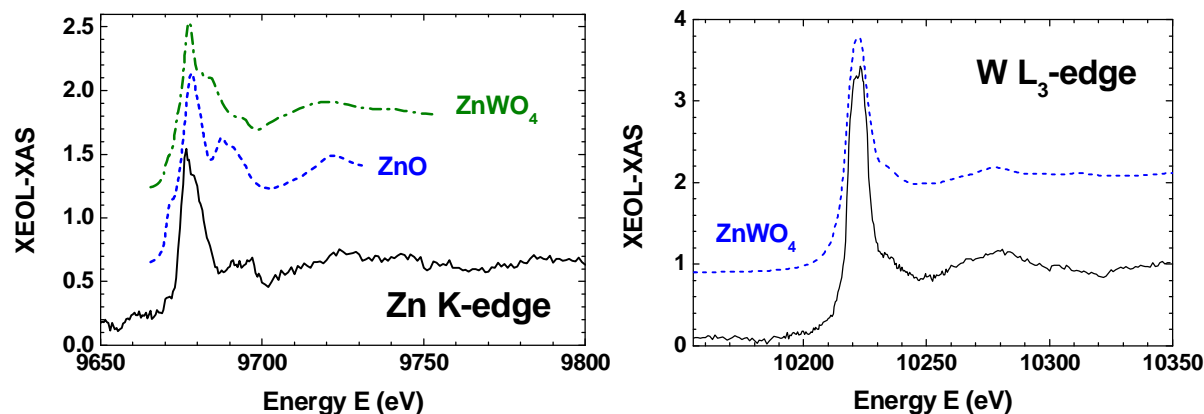


Figure 2 (Colour online) Zn K-edge and W L_3 -edge XANES signals (solid lines) measured through the SNOM probe, kept at the same position in near-field condition. Theoretically calculated Zn K-edge XANES signals in ZnO (dashed line) and $ZnWO_4$ (dash-dotted line) are shown for comparison in the left panel. The W L_3 -edge XANES signal for polycrystalline $ZnWO_4$, recorded in transmission macro-mode in [12], is shown by dashed line in the right panel. It is dominated by the “white line” peak, located at ~ 10222 eV.

and/or W absorption edges. A set of XEOL spectra was collected using the spectrometer and the LN-cooled CCD camera in the range from 300 nm to 800 nm for each fixed x-ray energy. Finally, the x-ray absorption spectrum was obtained plotting the XEOL spectra intensity at the wavelength of 500 nm (i.e. at the maximum of the photoluminescence band) as a function of the x-ray energy (figure 2). This spectrum is conventionally called x-ray absorption near edge structure (XANES) signal. Typical acquisition time for the single XANES signal was about 40 minutes. The obtained XANES signals were compared with the experimentally measured W L_3 -edge XANES in polycrystalline $ZnWO_4$, taken from [12] and theoretically calculated Zn K-edge XANES for ZnO and $ZnWO_4$ (see below).

In the second type of experiments, the prototype was operating in a conventional scanning mode, providing simultaneously the topographic and optical images (figure 3). The last one was collected by the SNOM probe in near-field condition and corresponds to the XEOL intensity variation at the wavelength 500 nm for the fixed x-ray energy. In this case, the XEOL signal was measured by an analogue PMT detector, and the x-ray energy was chosen below or above the Zn/W absorption edge to maximize the variation of the XEOL signal and, thus, to obtain the largest contrast in the optical image. We found that in our samples, the highest contrast is achieved by tuning x-ray energy at the W L_3 -edge “white line” maximum, located at ~ 10222 eV just above the edge (figure 2).

Full-multiple-scattering (FMS) calculations were performed in dipolar approximation ($\Delta l = \pm 1$) for ZnO and $ZnWO_4$ at the Zn K-edge using ab initio self-consistent FEFF8.0 code [13]. The clusters of up to 8 Å radius, having wurtzite-type ZnO or wolframite-type $ZnWO_4$ structure [14], were constructed around the central zinc atom (absorber). The muffin-tin cluster potential was calculated in a self-consistent way within a smaller cluster size of 4.0 Å for ZnO and 4.6 Å for $ZnWO_4$. The complex exchange-correlation potential (ECP) of Hedin-Lundqvist type was used to account for inelastic losses of the photoelectron. The final excited state was approximated by a fully relaxed configuration with a core hole at the Zn $1s$ -level and an additional electron in the Zn $4p$ -level. The constant core-hole related broadening of 1.897 eV was added to the complex part of the ECP. The XANES signals calculated for the largest cluster size 8 Å are shown in figure 2 (left panel) by dashed (for ZnO) and dash-dotted (for $ZnWO_4$) lines. The main difference between two XANES signals is observed above the first absorption maximum, located at ~ 9678 eV, and is related to different local environment of zinc atoms in two compounds.

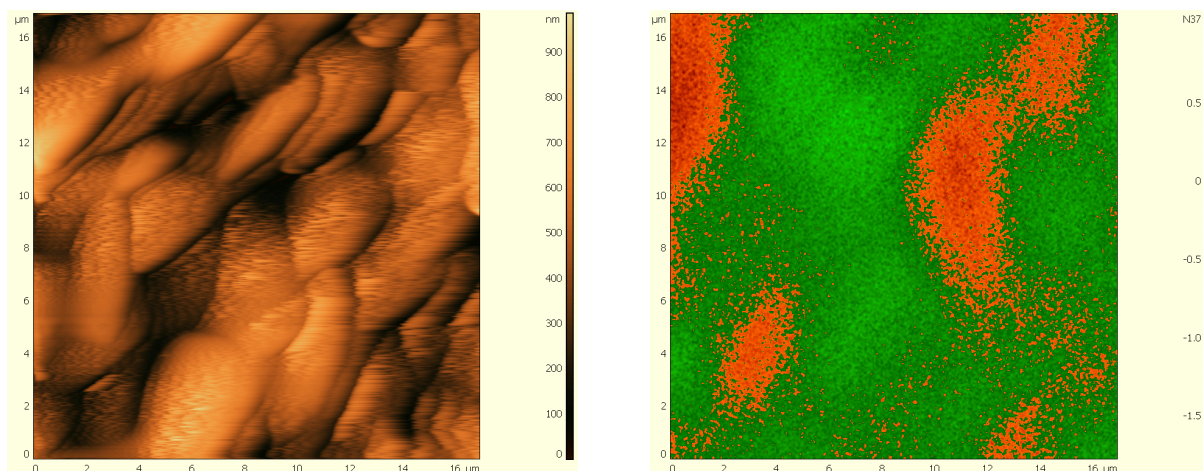


Figure 3 (Colour online) Topographic (left) and XEOL (right) images (size XYZ = $17\ \mu\text{m} \times 17\ \mu\text{m} \times 1000\ \text{nm}$) measured simultaneously in mixed ZnO-ZnWO₄ thin film sample. XEOL was excited at the W L₃-edge “white-line” maximum (10222 eV). Non-homogeneous distribution of tungsten rich regions (shown in red) is well observed in XEOL images.

3. Results and discussion

The results of the first-type experiment, presented in figure 2, show that the x-ray absorption spectra at the Zn K-edge and W L₃-edge can be recorded through the SNOM probe in near-field mode with a rather high signal-to-noise ratio.

As it was stated before, our thin film samples are composed of two crystallographic phases – ZnO and ZnWO₄. Therefore, one can expect that the XANES signal, measured at the W L₃-edge, reflects the local environment around tungsten atoms in ZnWO₄, whereas the Zn K-edge XANES represents a mixture of two signals, being due to zinc atoms located in ZnO and ZnWO₄ phases. The results in figure 2 confirm these conclusions. In fact, a comparison of the W L₃-edge XANES spectra, measured in near-field mode, with that, obtained for polycrystalline ZnWO₄ in transmission mode in [12], indicates their great similarity: both signals consists of the strong “white line” maximum, being due to the dipole-allowed transition $2p_{3/2}(\text{W}) \rightarrow 5d(\text{W})$ [15] and located at $\sim 10222\ \text{eV}$, and a fine structure above it, related to the excited photoelectron scattering by the surrounding atoms.

In the case of the Zn K-edge, the comparison was performed with theoretical XANES signals, calculated for ZnO and ZnWO₄ structures. One can see in figure 2 that in both structures the maximum in absorption occurs immediately above the edge at $\sim 9678\ \text{eV}$. However for higher x-ray energies, the behaviour of the two theoretical XANES signals is different. There is a peak between 9690 eV and 9700 eV in ZnO, whereas a minimum exists in ZnWO₄ signal. The quality of the experimental spectra and the limitations of the theoretical signals do not allow a precise analysis. Nevertheless, it is clear that experimental XANES signal does not agree separately with no one of the calculated signals. This fact confirms again the presence of two phases, which are mixed at a level significantly below the lateral resolution of the prototype (100 nm).

The high intensity of the W L₃-edge “white line” was used in the second-type experiments, in which topographic and optical (XEOL) images were simultaneously acquired. Figure 3 shows the result for non-homogeneous thin film sample, made of large grains with heights up to one micron and a RMS surface roughness of about 149 nm. The optical image, reflecting the intensity of the XEOL signal excited at the W L₃-edge “white line” energy, provides the distribution map of tungsten-rich and tungsten-poor regions or, to be more rigorous, the distribution of luminescent centres on the sample surface. In fact, it is not necessarily true that the emission efficiency is directly proportional to

the tungsten concentration, even if these two parameters are ultimately related to each other. From the optical XEOL image, tungsten-rich regions turn out to be as small as a few microns. This type of measurements provides a nanoscale optical contrast inherently related to the chemical distribution of the surface luminescent sites, thus extending the capabilities of conventional SNOM microscopes.

4. Conclusions

A new experimental XAS-SNOM technique, combining x-ray absorption spectroscopy using synchrotron radiation microbeams with scanning near-field optical microscopy has been established and its capabilities have been explored using two types of experiments. We showed that it is possible to measure full XANES signal through the SNOM tip, being in a fixed point at the sample surface with lateral resolution of the optical probe. It is also possible to perform simultaneous topography and XEOL scanning and to detect contrast in XEOL signal related to the absorption edge of an element. The developed technique is a promising tool to study x-ray luminescent nanoobjects. However, deeper understanding of the possibilities and limitations of the technique requires further investigations.

Acknowledgments

This work was partially supported by the European Commission through the FP6 STREP Project "X-TIP" (Contract No. NMP4-CT-2003-505634). The financial support by INFM (Italy) is acknowledged. Authors are grateful to the staff of the ID03 beamline for assistance during the measurements.

References

- [1] Rehr J J and Ankudinov A L 2005 *Coord. Chem. Rev.* **249** 131
- [2] X-ray Absorption: Principles, Applications, Techniques of EXAFS, SEXAFS, and XANES, in *Chemical Analysis* **92**, ed. D C Koningsberger and R Prins (John Wiley & Sons, 1988)
- [3] X-Ray Spectrometry: Recent Technological Advances, ed. K Tsuji, J Injuk, R Van Grieken (John Wiley & Sons, 2004)
- [4] Mimura H, Matsuyama S, Yumoto H, Hara H, Yamamura K, Sano Y, Shibahara M, Endo K, Mori Y, Nishino Y, Tamasku K, Yabashi M, Ishikawa T and Yamauchi K 2005 *Jpn. J. Appl. Phys.* **44** L539
- [5] Hignette O, Cloetens P, Morawe C, Ludwig W, Bernard P, Rommeveaux A and Bohic S 2007 *AIP Conf. Proc.* **879** 792
- [6] Bilderback D H, Hoffman S A and Thiel D J 1994 *Science* **263** 201
- [7] Snigirev A, Bjeoumikhov A, Erko A, Snigireva I, Grigoriev M, Erko M and Bjeoumikhova S 2007 *J. Synchrotron Rad.* **14** 227
- [8] Jarre A, Fuhse C, Ollinger C, Seeger J, Tucoulou R and Salditt T 2005 *Phys. Rev. Lett.* **94** 074801
- [9] Kang H C, Maser J, Stephenson G B, Liu C, Conley R, Macrander A T and Vogt S 2006 *Phys. Rev. Lett.* **96** 127401
- [10] Schroer C G, Kurapova O, Patommel J, Boye P, Feldkamp J, Lengeler B, Burghammer M, Riekel C, Vincze L, van der Hart A and Kuchler M 2005 *Appl. Phys. Lett.* **87** 124103
- [11] Hecht B, Sick B, Wild U P, Deckert V, Zenobi R, Martin O J F and Pohl D W 2000 *J. Chem. Phys.* **112** 7761
- [12] Kuzmin A and Purans J 2001 *Rad. Measurements* **33** 583
- [13] Ankudinov A L, Ravel B, Rehr J J and Conradson S D 1998 *Phys. Rev. B* **58** 7565
- [14] Galasso F S 1970 *Structure and Properties of Inorganic Solids* (Pergamon Press, Oxford)
- [15] Kuzmin A and Purans J 1993 *J. Phys.: Condens. Matter* **5** 9423